Catal Lett (2011) 141:592–601
DOI 10.1007/s10562-011-0546-x

Glycothermal Synthesis and Catalytic Properties of Nanosized $Zn_{1-x}Co_xAl_2O_4$ ($x = 0$, 0.5, 1.0) Spinels in Phenol Methylation

Wiktoria Walerczyk · Mirosław Zawadzki · Hanna Grabowska

Received: 23 June 2010 / Accepted: 4 January 2011 / Published online: 15 January 2011

Abstract $Zn_{1-x}Co_xAl_2O_4$ ($x = 0$, 0.5, 1.0) spinels were synthesised under microwave-assisted solvothermal conditions using 1,4-butanediol as reaction medium. The results of XRD and HRTEM have indicated nanocrystallinity of prepared materials (average crystallite size in the range 6–16 nm), and N_2 adsorption–desorption measurements have revealed high feature of their surface area and mesoporous nature. Acid–base properties of prepared materials were determined using TPD-NH_3 method and cyclohexanol test. All studied spinels that underwent examination were active in phenol methylation but Co-substituted zinc aluminate ($Zn_{0.5}Co_{0.5}Al_2O_4$) was found to be the most efficient in the selective formation of *ortho*-methylated products. It could be ascribed to its dominant basic character and the presence of weak and strong acid centres, and the highest surface area as well.

Keywords Aluminate spinels · Glycothermal method · Phenol methylation

1 Introduction

Spinels are mixed oxides with general formula AB_2O_4, where A represents a divalent metal cation that usually occupies a tetrahedral site while B represents trivalent metal cation that normally occupies the octahedral sites of a cubic crystal structure. In normal spinel structure A^{2+} and B^{3+} occupy 8 tetrahedral and 16 octahedral sites, respectively, while in the inverse structure B^{3+} ions may occupy both octahedral and tetrahedral sites, depending on the degree of inversion. Moreover, so called random spinels are also possible in which there is statistical distribution of ions between both sites. The physico-chemical properties of spinels depend mainly on cations distribution and their nature which may be changed or modified by the introduction of the third metal to the spinel structure. Various substitutions may be incorporated into it, so adequate selection of substituting ion and appropriate chemical composition are of the utmost importance in order to achieve desired properties of material, including its catalytic performances. Synthesis method is also a significant factor influencing the properties of the obtained material such as crystallite size, specific surface area or porosity [1–3].

Common spinel compounds known as aluminate family, including $ZnAl_2O_4$, have been already studied as catalysts and catalysts' carriers because of their combination of desirable properties such as high mechanical resistance, high thermal stability, low sintering temperature, low surface acidity and high ability of cations diffusion. Therefore, they are mainly used as high temperature ceramics, but also as useful material for optical and catalytic applications. In our earlier studies we elaborated the high active aluminate catalysts, which enable obtaining methylated phenols [4], synthesis of 1-methylimidazole [5], and efficient methylation of 2- and 4-hydroxypyridine [6, 7].

Aluminates may be obtained by many different methods, e.g. solid state reaction (ceramic, mechanochemical) method [8] or wet chemical routs such as (co)precipitation [9], sol–gel [10], solvothermal methods [11] and some other methodologies like molten salts synthesis [12], combustion in various solutions [3], polymeric precursors method [13], etc. Glycothermal method, being one type of the solvothermal process, offers some advantages over

W. Walerczyk (✉) · M. Zawadzki · H. Grabowska
Institute of Low Temperature and Structure Research, Polish Academy of Sciences, Okólna 2, 50-422 Wrocław, Poland
e-mail: wiktoria.walerczyk@int.pan.wroc.pl

most other methods like short reaction time, the possibility of using various precursors and reaction media. Different reaction parameters such as pressure, temperature, synthesis time and even heating method can affect the reaction products [14]. Mixed oxides obtained by glycothermal synthesis are usually nanocrystalline materials with well-controlled chemical composition and very interesting textural properties (high surface area, mesoporosity) [15].

Phenol belongs to compounds characterised by high reactivity which alkyl derivatives can be obtained during alkylation with olefins or alcohols under relatively mild conditions in the liquid as well as gas phase. Usually, the reaction of phenol with methanol is performed in the gas phase in the presence of catalyst. Reaction conducted in the gas phase has many advantages especially when used catalyst is highly active and selective. In the process carried out in such a way the troublesome separation of reaction products is eliminated.

The most important commercial alkylphenols are the methyl derivatives (the cresols and xylenols); among them, *ortho*-cresol and 2,6-xylenol, belong to the most crucial because of their further applications. They are the most sought after for the further production of agrochemicals, antioxidants, plastics, pharmaceuticals, and very useful polymers, etc. There is always competition between C- and O-alkylation and the strength of acid centres profoundly affects the product selectivity [16]. The surface of catalysts should possess both basic and acidic (mainly Lewis) properties to secure a high yield of C-methylated phenol derivatives. The catalyst selectivity is attributed to a presence of acidic centres possessing weak and medium strength [17]. For catalysts exhibiting mainly Brönsted acidic sites, especially strong, the selectivity towards C-methylated products decreased with temperature [16]. It is accepted that only Brönsted acidity is responsible for coke formation. Suitable catalysts for the gas phase methylation of phenol with methanol have been reported in the literature. Catalysts having basic properties such as MgO [18–20] or Fe_2O_3-based [21–23] produce predominantly ring alkylated product*s* with high *ortho*-selectivity. With the increase in the acidity of catalysts, e.g. for Al_2O_3 or zeolites [24–26], the selectivity for C-alkylated products decreases and products of O-alkylation are obtained. Among active catalysts in the phenol methylation, materials with spinel structure are very interesting, e.g. ferrites [27–30] and also others [31–33]. Issues concerning the mechanism of phenol alkylation have been presented in many publications. Among them the works of Mathew et al. [28, 34–37] are worth to be quoted, in which the authors have presented a proposal for the mechanism of phenol methylation occurring on well-characterised spinel catalysts. They underlined the role of an acid–base pair sites as the active centres for the *ortho*-methylation reactions.

Some of the present authors have studied catalytic reaction of phenol with methanol leading to *ortho*-cresol and 2,6-xylenol in the presence of $ZnAl_2O_4$. It was stated that zinc aluminate was an active and selective catalyst in the alkylation of phenol and other hydroxyarenes [4, 6, 7, 38]. The catalytic properties in methylation of phenol of zinc aluminate with incorporation of different metals, e.g. copper and iron were also investigated [39, 40].

The aim of the present work was to study the effect of substitution of Zn^{2+} by other divalent cation, namely Co^{2+}, in the framework of zinc aluminate spinel on phenol conversion and *ortho*-methylated products selectivity during methylation. $Zn_{1-x}Co_xAl_2O_4$ ($x = 0$, 0.5, 1) spinels, prepared under microwave-assisted glycothermal conditions, were characterized using XRD, TEM/SEM, N_2 adsorption–desorption, TPD-NH_3 and CHOL test to find a relationship between the structure, acid–base properties and the catalytic behaviour.

2 Experimental

2.1 Samples Preparation

$ZnAl_2O_4$ (ZAO), $Zn_{0.5}Co_{0.5}Al_2O_4$ (ZCAO) and $CoAl_2O_4$ (CAO) were prepared from the following precursors: zinc acetate, $Zn(CH_3COO)_2{\cdot}2H_2O$ (POCH Poland); cobalt acetate, $Co(CH_3COO)_2{\cdot}2H_2O$ (POCH Poland); and aluminium isopropoxide, $Al[OCH(CH_3)_2]_3$ (Alfa Aesar) mixed in molar ratio 1:0:2, 1:1:4, 0:1:2, respectively. First, appropriate amount of zinc and/or cobalt acetates were dissolved in water, and aluminium isopropoxide was suspended in 99% 1,4-butanediol $HO(CH_2)_4OH$ (Alfa Aesar). Then solutions of metals precursors were mixed together and put in a Teflon vessel placed in an autoclave with microwave heating (MW Reactor, Ertec, Poland). Synthesis time was set up to 60 min and reaction was provided at 200 °C under autogenic pressure of $\sim$25 atm. Reaction products were washed with acetone and centrifuged; this procedure was repeated several times to remove residues of organic compounds. After that, products were extruded and obtained wires were air dried at 70 °C, crushed and then calcined at 550 and 1100 °C for 3 h.

2.2 Characterization Methods

Phase identification of obtained materials, as-prepared and after heat treatment were analysed using Powder X-Ray Diffraction. XRD measurements were performed by X'Pert Pro Panalytical diffractometr with Cu Kα radiation

($\lambda = 1.5406$ Å). XRD data and Scherrer equation were used to average grain size calculation.

Samples morphology and microstructure were analysed by High Resolution Transmission Electron Microscopy (HRTEM) and Selected Area Electron Diffraction (SAED). HRTEM images and SAED patterns were recorded on Philips CM 20 SuperTwin microscope operated at 200 kV with 0.25 nm resolution. Studied materials were grinded in mortar, suspended in methanol, and dispersed ultrasonically. One drop of suspension was placed on a copper grid covered with performed carbon and allowing the solvent to evaporate, then specimen were dried and placed in the microscope.

The morphology of samples was also observed with the use of Scanning Electron Microscopy (SEM) and elemental analysis was made by using Energy Dispersive X-ray Spectroscopy (EDS). The measurements were carried out on SEM 515 Philips Scanning Electron Microscope equipped with EDAX.

Textural properties including porosity and specific surface area were calculated from N_2 adsorption–desorption isotherms obtained at liquid nitrogen temperature. The measurements were carried out on a Autosorb-1 Quantachrome Instruments automated system. Prior to measurements samples were degassed under vacuum at 200 °C for 2 h. The adsorption data were interpreted by the application of the conventional Brunauer–Emmet–Teller (BET) method for the determination the specific surface area S_{BET}. The Barret–Joyner–Halenda (BJH) method was employed for pore size distribution calculations. The mean pore size (D) corresponds to maximum of pore size distribution curve.

The total surface acidity and the acid strength distribution were investigated by the Temperature-Programmed Desorption of ammonia (TPD-NH_3) method. Before the measurements, the samples (2 g) were firstly heated from room temperature to 550 °C in argon flow for 1 h and next cooled to 180 °C. After cooling the samples adsorption of pure ammonia was performed for 0.5 h followed by a purge with argon at 180 °C for 1 h to remove physically adsorbed NH_3. Finally, TPD-NH_3 measurements were started in argon with a heating rate of 10 deg/min. Amounts of desorbed ammonia were analysed using a gas chromatograph with a TCD detector.

Reaction of cyclohexanol (CHOL) decomposition was chosen to determine acid–basic properties of obtained materials. Both acid and basic centres are responsive for cyclohexanol dehydrogenation to cyclohexanone (CHON), whereas cyclohexanol reacts on acid centres to cyclohexene (CHEN). Literature data suggest that decomposition to CHEN is the measure of the surface's acid strength while CHON/CHEN selectivity ratio gives information about basic nature of materials [41]. The measurements of catalytic activity in cyclohexanol decomposition were carried out in a continuous-flow fixed bed quartz reactor with electric heating. The catalyst (0.1 g) mixed with SiC (to 1 cm^3 volume) was held on quartz wool. During reaction total gas flow was set on 10 dm^3/h (dry N_2 99.999% saturated with CHOL—2.6 mmol/h) and reaction temperature was fixed at 300 °C. Reaction products were analysed using gas chromatograph equipped with FID detector. Total conversion of CHOL and both yields and selectivities to CHEN and CHON were calculated.

2.3 Catalytic Methylation of Phenol

Alkylation of phenol with methanol was performed in a continuous manner by a conventional flow method at atmospheric pressure without added carrier gas. The reactions in the presence of ZAO, ZCAO and CAO were carried out using an electrically heated standard down flow fixed-bed vertical quartz reactor of 6 mm inner diameter filled with 3 cm^3 of catalyst (0.6–1.2 mm particle size). The space below catalyst bed was filled with quartz wool. The temperature of the bed was continuously controlled with a thermocouple placed inside the catalyst bed. A solution of phenol in methanol with an addition of water (molar ratio 1:5:1, respectively) was introduced to the reactor from the top at pre-determined flow rate equal 1.5 cm^3/h (load 0.5 h^{-1}) by a micro-feed syringe pump. Water was added to the aromatic–alcohol mixture of reactants to prolong the activity of the catalysts during the reaction of methylation [28, 42–44]. It is suggested that the addition of water into the substrates mixture lowers coke deposition on the catalyst surface and the share of side reactions is decreased as well [43]. The reaction conditions were reducing, since the optimal methanol to phenol ratio used was 5, far exceeding the nominal value of 2 from reaction of phenol with methanol stoichiometry leading to synthesis of 2,6-xylenol. A large excess of methanol is used to secure high conversion of phenol and due to its lost by decomposition during reaction of methylation and is necessary due to weak interaction of MeOH to the catalyst surface [36]. The alkylation reactions were studied continuously as a function of increasing temperature from 220 up to 360 °C. Before the proper experiments catalysts were activated during 2 h in the flow of the reactants mixture at temperature up to 200 °C. The experiments were carried out for 1–2 h under steady conditions at chosen temperatures. The reactant mixture was evaporated and preheated to the reaction temperature in the upper part of the reactor before it entered the catalyst bed. Liquid reaction products, along with unreacted substrates, were collected in a trap below the catalytic bed and analysed by a HP 6890 gas chromatograph equipped with a FID detector and a capillary column (30 m × 0.32 mm × 0.25 μm) filled with 5%

phenyl methyl silicone. Helium was used as a carrier gas. The identification of products was carried out by the comparison of their retention times to the known standards. The conversion of phenol was defined as a fraction of reacted phenol, whereas the selectivity was obtained on the basis of the percentage of the given alkyl phenols (*ortho*-cresol and 2,6-xylenol) in the liquid reaction products. The total *ortho*-selectivity was defined as a sum of the selectivities towards *ortho*-cresol and 2,6-xylenol. Gases formed during reaction, such as CO, CO_2, CH_4 and H_2 were not analysed.

3 Results and Discussion

3.1 Characterisation Results

XRD measurements confirm spinel structure of samples heated at 550 (Fig. 1) and 1100 °C (not shown). XRD patterns of ZAO and ZCAO samples exhibit peaks characteristic only for spinel structure of $ZnAl_2O_4$ (JCPD 05-0669). Data obtained from measurement of CAO sample indicate $CoAl_2O_4$ (JCPD 38-0814) and a small amount of the second phase presence. Additional diffraction peak at $2\Theta = 42.4°$, unmatched to spinel structure of $CoAl_2O_4$, is very weak suggesting low content of this phase. It could originate from (200) lattice plane of cubic system of CoO (JCPD 43-1004) but there is no other evidence on this thesis because HRTEM images and SAED patterns did not further confirm its presence. Scherrer equation and XRD measurements were being used to calculated average crystallite size (d^{av}_{XRD}) and lattice parameters, and the results are presented in Table 1. The average crystalllite sizes of samples heated at 550 °C amounted 6 nm for ZAO as well as for ZCAO, and 16 nm for CAO sample evidencing the nanometer character of the prepared spinels. After heat treatment at 1100 °C, there are greater differences between average crystallite sizes (21, 37, 44 nm for ZAO, ZCAO and CAO, respectively), which indicate better thermal stability of ZAO sample. Analysis of XRD profiles of studied samples suggests also different crystallite size distribution for CAO sample than for others. In this case, diffraction peaks could be approximate by Lorentz profile what is characteristic for materials with a wide distribution in the size of crystallites. The data included in Table 1 also show that all prepared spinels had characteristic cubic structure but an increase of lattice parameters (unit-cell parameter and volume) due to Co incorporation into zinc aluminate lattice was noticed for ZCAO and CAO samples. Considering the ionic radii for 4-coordinated Zn^{2+} (0.060 nm) and Co^{2+} (0.058 nm) as well as 6-coordinated Al^{3+} (0.0535 nm) and Co^{3+} (0.065 nm), one can expect the Co substitution for tetrahedral sites resulting in decrease of lattice parameters. However, the observed lattice expansion (more pronounced for samples heated at 1100 °C) indicates that some amount of Co^{2+} should be in octahedral sites leading to considerable level of inversion of spinel structure. Such trend of $ZnAl_2O_4$ lattice expansion due to Co doping has already been reported in the literature by Popović et al. [45]. Thought, the general formula for ZCAO sample can be written as $^{IV}[Zn_{0.5}Co_{0.5-\delta}]^{VI}[Al_{2-\delta}Co_{\delta}]O_4$, where δ is the inversion parameter of the spinel structure.

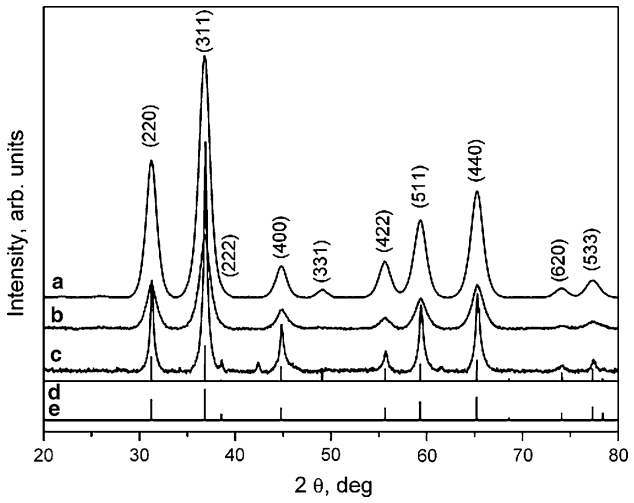

Fig. 1 XRD patterns of spinels prepared by the glycothermal method: (*a*) ZAO, (*b*) ZCAO, (*c*) CAO, and JCPDS data for (*d*) $ZnAl_2O_4$ (No. 05-0699) and for (*e*) $CoAl_2O_4$ (No. 38-0814)

Table 1 Structural and textural properties of studied spinels

Sample	ZAO		ZCAO		CAO	
$T_{calc.}$ (°C)	550	1100	550	1100	550	1100
d^{av}_{XRD} (nm)	6	21	6	37	16	44
Latice parameters						
a (Å)	8.0799	8.0795	8.0812	8.086	8.0821	8.1012
α (°)	90	90	90	90	90	90
V (Å^3)	527.49	527.77	527.75	530.60	527.93	531.67
S_{BET} (m^2/g)	107	40	152	18	113	18
V_{BJH} (cm^3/g)	0.19	0.08	0.32	0.12	0.26	0.12
D_{pores} (nm)	6.5	8.1	6.6	17.3	7.8	12.2

Representative micrographs of HRTEM images of ZAO, ZCAO and CAO samples are shown in Fig. 2a, b and c, respectively. For ZAO sample, there are well visible small particles with narrow size range of crystallite where d^{av}_{TEM} amounted 4.1 nm. ZAO particles have rather spherical shape and lattice fringes with distance about 0.29 nm characteristic for (220) lattice plane of zinc aluminate spinel structure. SAED patterns obtained from this sample show broadening of diffraction rings indicating low

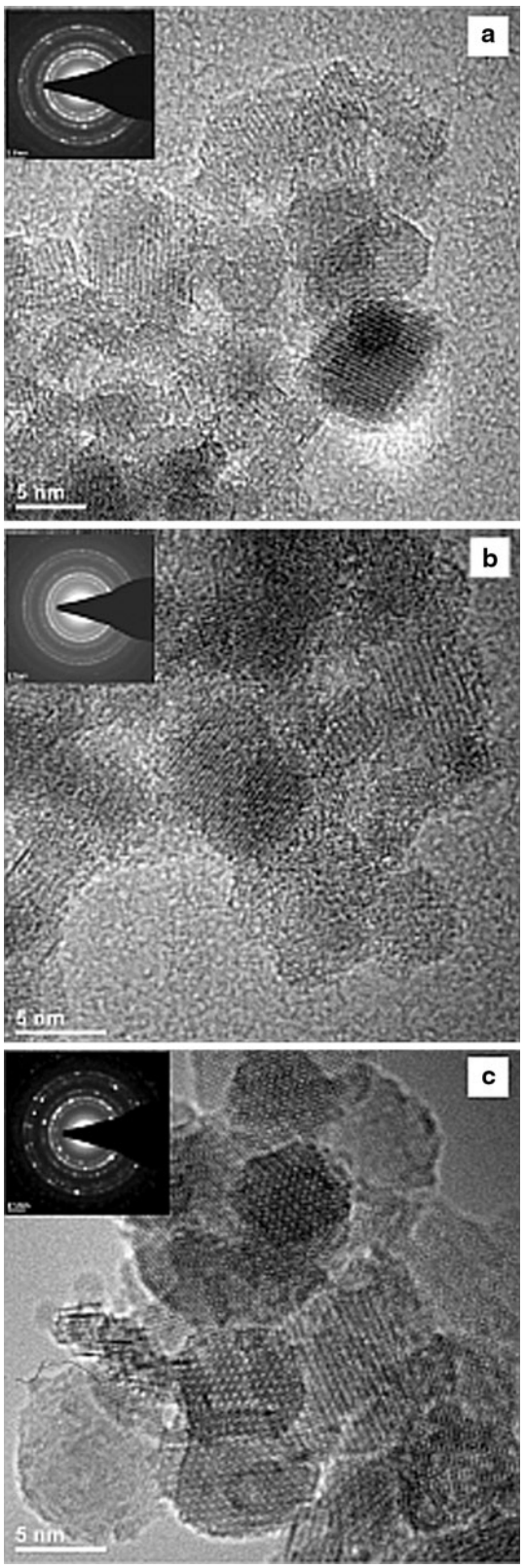

Fig. 2 HRTEM images of (**a**) ZAO, (**b**) ZCAO and (**c**) CAO spinels with SAED patterns shown as *insets*

crystallinity. Diffraction rings with lattice distances 0.291, 0.244, 0.203, 0.158 and 0.143 nm could be assigned to (220), (311), (400), (511) and (440) lattice plane of cubic $ZnAl_2O_4$ structure, respectively. HRTEM images of ZCAO are similar to the ZAO one. Small spherical crystallites of size in the range 4–8 nm were noticed. SAED patterns of ZCAO sample also present broad diffraction rings with lattice distance characteristic only for $ZnAl_2O_4$ without impurities. The morphology of CAO sample is less uniform, particles with different shape and size are visible but most of them are quasispherical with diameter in the range 7–18 nm and d^{av}_{TEM} amounts of 8.5 nm. The presence of sliver crystals with 30 nm of the length, 3 nm of the breadth and lattice fringes could be noticed on some images of CAO sample which might be assigned to Co_3O_4 (JCPDS 42–1467) as well as to $CoAl_2O_4$ structure. SAED patterns of CAO sample contain only rings corresponding to the cobalt aluminate with well visible individual spots attributed to large crystals. It confirms spinel structure of CAO sample and higher crystallinity of this material in comparison to ZAO and CAO sample. HRTEM images recorded on the samples heated at 1100 °C (not shown) reveal significant increase in particle sizes (corresponding particle size distributions become broader) but nanocrystalline nature of the samples is still preserved. SAED measurement has shown that particles are well crystallized and diffraction rings match the corresponding XRD peaks.

SEM images (not shown) reveal that there are no significant differences between prepared spinel samples, and all of them consist of characteristic agglomerates of irregular shape. For all spinels, EDS analysis confirmed that atoms content is in a good agreement with the scheduled one.

Taking into account the nitrogen adsorption–desorption isotherms, displayed in Fig. 3, and the calculated values of both the specific surface area S_{BET} and the pore diameter D, listed in Table 1, one can see that all prepared spinels are typical mesoporous materials. The isotherms are of type IV and show the hysterisis loop of H1/H2 type what is characteristic for mesoporous materials, according to IUPAC classification. Such a shape of isotherms is typical for materials consisting of particles crossed by nearly cylindrical channels or spheroidal particles formed in agglomerates or aggregates, in which pores can have uniform (type H1) or nonuniform size and shape (type H2). It should be noted that the nitrogen isotherms show a sharp increase of adsorbed nitrogen volume at high partial pressures ($P/P_o \sim 0.6$) which corresponds to a large mesopore volume with a relatively narrow distribution of pore diameters in the range 2–20 nm with a maximum at ~6–8 nm. This type of sorption properties has been pre-

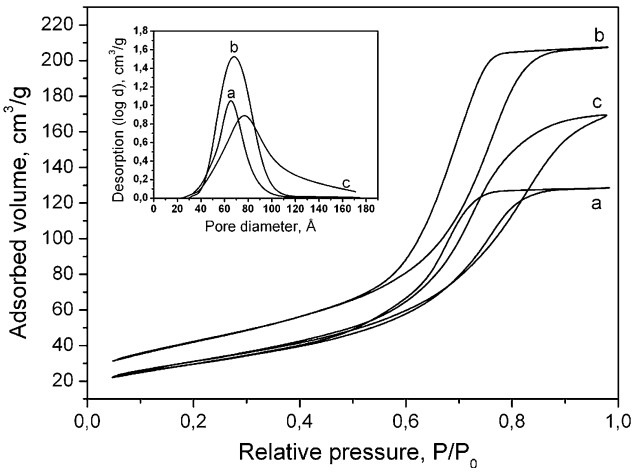

Fig. 3 N_2 adsorption–desorption isotherms of (*a*) ZAO, (*b*) ZCAO, (*c*) CAO spinels with corresponding pore size distributions (as an *inset*)

viously reported for nanosized crystalline or amorphous materials and was attributed to interparticle mesoporosity [46, 47]. The data listed in Table 1 show that ZCAO sample exhibits the higher surface area and pore volume than others, which could be a result of the numerous surface defects caused by substitution Zn by Co ions. Heat treatment at 1100 °C leads to decrease of specific surface area and increase of pore diameter for all examined samples but ZAO maintained significant value of S_{BET}, i.e. 40 m^2/g, and D was changed a little. N_2 adsorption–desorption measurements exhibited that microwave-assisted glycothermal method is useful to prepare spinels with appropriate textural properties for materials used as catalysts or catalyst supports.

Total acidity and strength distribution of acid sites were estimated from measurements of NH_3 thermodesorption

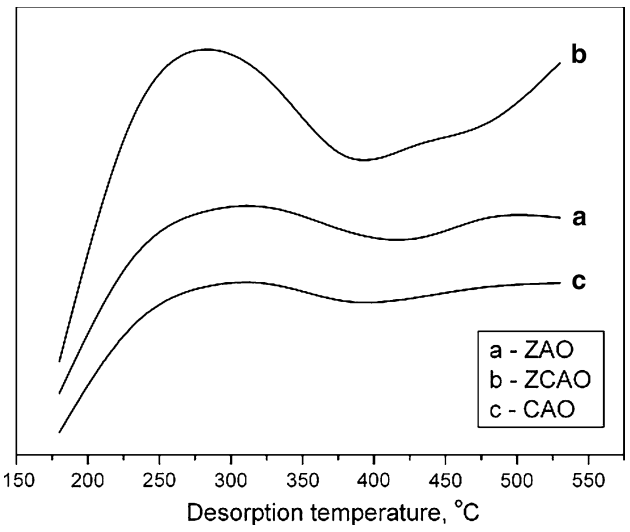

Fig. 4 TPD-NH_3 profiles for spinel samples

(Fig. 4). The highest acidity exhibits ZCAO (1.2 mmol NH_3/g) while ZAO and CAO samples show much lower and comparable total acidity, respectively 0.73 and 0.62 mmol NH_3/g. The acid strength distribution shows that ZCAO sample has higher part of weak ($T_{des} < 300$ °C) and strong acid sites ($T_{des} > 500$ °C) than ZAO and CAO, but lower part of the medium ones.

CHOL test specifies the acid–base properties of the studied materials. Results of CHOL decomposition are collected in Table 2. Tests of CHOL conversion show that ZCAO sample is the most active among examined materials exhibiting also the highest selectivity to CHON and the lowest selectivity to CHEN what indicates on dominate basic character of this sample. The lower conversion of cyclohexanol is observed for CAO sample. Selectivity to CHEN for ZAO and CAO is similar and confirms results obtained from TPD-NH_3. However, it should be noticed that the selectivity to CHON indicates rather basic character of the CAO surface and rather equal content of acid and basic centres in the case of ZAO sample. Differences in results obtained in CHOL conversions between ZCAO and the other studied samples are probably due to the changing of spinel surface caused by the partial substitution of Zn by Co ions. It is well known that the acid–base properties of spinel-type compounds depend on the extent of polarity of the metal cation and the oxygen anion, respectively. Besides, Jacobs et al. [48] have previously revealed that octahedral sites are exposed almost exclusively at the spinel surface: for $ZnAl_2O_4$ and $CoAl_2O_4$ non or only a very small amount of Zn and Co, respectively, were detected by LEIS at the spinel surface. It may suggests dominant role of octahedral sites in determining the surface acidity/basicity. Supposing that only a part of Co^{2+} ions substitute for Zn^{2+} on tetrahedral sites, and the remaining cobalt ions substitutes for Al^{3+} on octahedral sites (simultaneously removing Al^{3+} ions to tetrahedral sites) it would be expected that the nature of active centres of ZCAO should be different. Moreover, for zinc aluminate substituted by other transition metal ions, e.g. for $Zn_{1-x}Mn_xAl_2O_4$, the oxidative transfer of Mn^{2+} in the tetrahedrally coordinated sites to Mn^{3+} in octahedral positions takes place what is reflected by its catalytic activity [48].

Table 2 Results of CHOL decomposition over studied spinels

Sample	ZAO	ZCAO	CAO
Conversion of CHOL[a] (%)	61.5	74.9	25.8
Selectivity to CHEN[b] (%)	29.3	5.2	25.3
Selectivity to CHON[c] (%)	68.4	94.8	74.7
CHON/CHEN	2.3	18.2	3.0

[a] Cyclohexanol

[b] Cyclohexene

[c] Cyclohexanone

3.2 Catalytic Performance

The course of the phenol methylation on studied catalysts was examined as a function of temperature under the same conditions. The influence of the reaction temperature upon the conversion, main reaction products yields and *ortho*-selectivity were investigated. The major methylated reaction products were found to be anisole, *ortho*-cresol and 2,6-xylenol. Except for these methyl derivatives, in the reaction products other compounds were also found. It was established that in this group traces of *meta*- and *para*-cresols, isomeric xylenols, higher methylated methylphenols, methyl substituted anisole and some amounts of other compounds, which had not been identified, were also present.

Figure 5 shows changes in the catalytic activity of the spinel catalysts with process temperature. One can conclude that all studied materials are active in the reaction of phenol methylation. Conversion of phenol for all catalysts increases significantly with temperature increasing. The higher initial activity was obtain for ZCAO and CAO, i.e. cobalt containing aluminate spinels. These spinels among tested catalysts exhibited an efficient activity without decay; the phenol conversion was growing up to 320 °C reaching in both cases higher level than 95%. After further increase of reaction temperature the activities of ZCAO and CAO remained on almost the same level. In the presence of ZAO catalyst the phenol conversion reached only about 50% at 340–350 °C, then it was visible lower. Over all studied catalysts, after stopping the reaction, cooling down, and starting all over again, almost the same conversions were attained at the same temperatures, as previously had been observed.

The yields of main methylated products obtained during alkylation reaction in relation to temperature over studied catalysts are illustrated in Fig. 6. Mainly C-methylated products at *ortho* positions were obtained, however, O-alkylation leading to anisole also occurred and its yield reached the highest value (~26%) when as catalyst CAO sample was used while the lowest phenol conversion to anisole was observed over ZAO catalyst. Shape of all curves indicate that yield of anisole declines when temperature is increased suggesting that anisole is not a side product but the intermediate which undergoes the rearrangement giving *ortho*-cresol and also phenol as a demethylation product [49]. As seen in Fig. 6 all catalysts are active in C-methylation at *ortho* positions to hydroxyl group of phenol ring. Parallel with *ortho*-cresol formation 2,6-xylenol was formed. Zinc aluminate (ZAO) in the reaction conditions exhibited the lowest conversion to anisole, on the other hand, it was also the least effective catalyst for *ortho*-alkylation at 2- and 2,6-positions. In its case the maximal value of sum of yields of *ortho*-cresol and 2,6-xylenol achieved up to 34% only at 340 °C while for the CAO catalyst it reached 41% at temperature lower by 60 degree. The best efficiency, in comparison to other spinels, was exhibited by ZCAO catalyst which allowed to obtain about 24% of *ortho*-cresol at 280 °C and up to 54% of 2,6-xylenol at 360 °C. It should be noted that in the presence of ZCAO catalyst C-methylation reaction has a

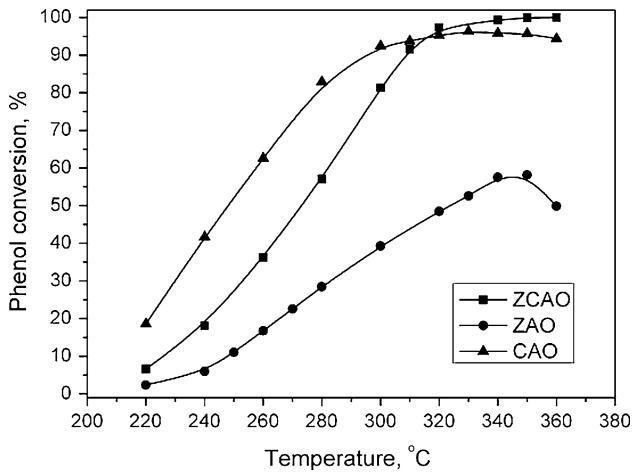

Fig. 5 Comparison of phenol conversions over glycothermally synthesised spinels in methylation reaction

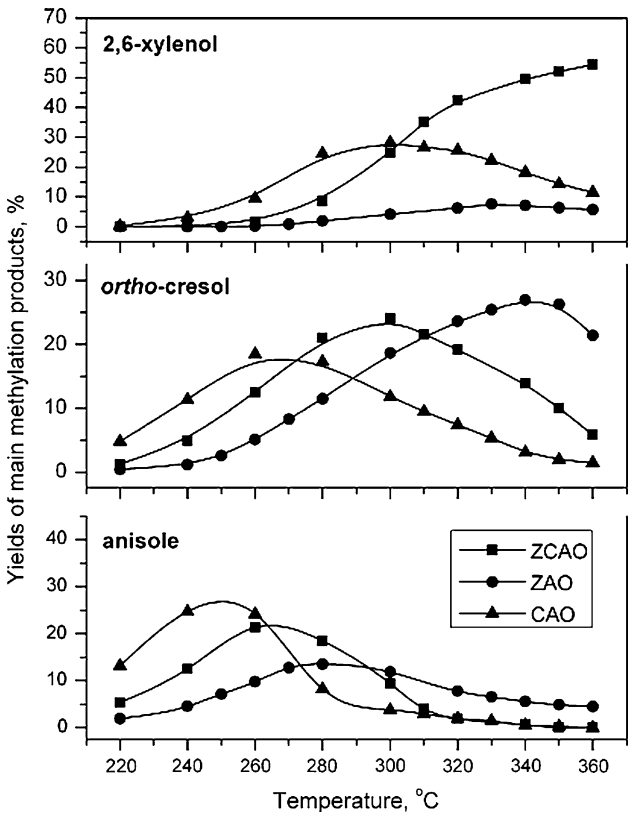

Fig. 6 Temperature dependence of yields of main methylation products obtained for ZAO, ZCAO and CAO catalysts

consecutive character. First, *ortho*-cresol was formed and then 2,6-xylenol as a result of subsequent reaction.

Figure 7 summarizes data of *ortho*-selectivity for phenol methylation over all the studied catalysts obtained as the effect of temperature. The selectivity towards *ortho*-cresol and 2,6-xylenol are shown and additionally the curves for total *ortho*-selectivities were also plotted. It should be noted that the highest selectivity to both *ortho*-methylated products was obtain when ZCAO was used as a catalyst. In this case the total *ortho*-selectivity increased with temperature reaching a maximal value (above 62%) at 310 °C which remained nearly on the same level with further increases of reaction temperature. It was observed that this catalyst possessing zinc as well as cobalt cations led to increase in the rate of consecutive methylation of the initially formed *ortho*-cresol, causing higher selectivity towards 2,6-xylenol. In the case of ZAO catalyst similar high value of selectivity was obtained, to the *ortho*-methylated phenol derivatives, as in the case of ZCAO. The catalyst with the lowest activity and *ortho*-selectivity has established to be a CAO, for which significant decrease in *ortho*-selectivity was observed when reaction temperature was increased. The comparison of catalytic behaviour of studied catalysts shows that Co-modified zinc aluminate is the most efficient (active and *ortho*-selective) in studied reaction.

The effect of contact time on phenol conversion and the main methylation products selectivities was studied in order to confirm the observed reaction sequence during alkylation. It was investigated by varying the feed rate over ZCAO catalyst at 260 °C and the results are presented in Fig. 8. Anisole and *ortho*-cresol are primary alkylation products since both are formed at the onset of the reaction. As the contact time increases, the selectivity of anisole decreases while the selectivity of *ortho*-cresol increases first, attains the maximum value and then decreases. The formation of 2,6-xylenol was favored by a large contact time and may occur by the direct C-alkylation of phenol via *ortho*-cresol or from anisole. The shape of the curves in Fig. 8 indicates that anisole is responsible to a large extent for the secondary products: at lower contact time, anisole initially formed undergoes an intramolecular rearrangement and may act as methylation agent for phenol to give *ortho*-cresol while at higher contact time, it undergoes further methylation to give 2,6-xylenol. It has become clear since the reaction temperature was increased, anisole selectivity decreased indicating that secondary reactions of anisole were suppressing. It seems that phenol methylation over ZCAO, and probably over other studied catalysts, is possible via both pathways, i.e. direct methylation and through anisole as the intermediate.

Catalytic properties of materials are determined by the type and quality of active centres. Acid–base properties of catalysts' surface play a crucial role in the reaction of phenol methylation. These properties of applied catalysts should be taken into account to explain their activity, products distribution and selectivity in studied reaction.

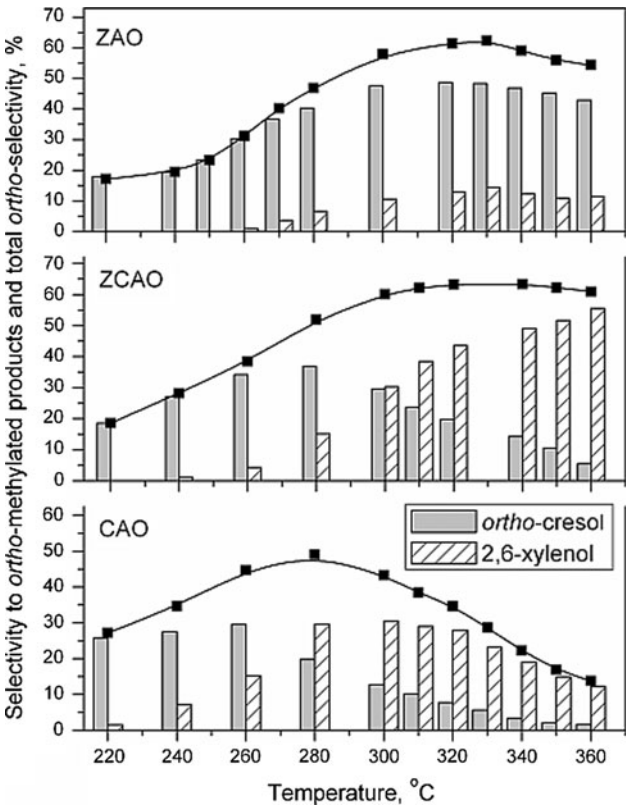

Fig. 7 Comparison of selectivities towards formation of *ortho*-cresol and 2,6-xylenol and total *ortho*-selectivity for ZAO, ZCAO and CAO catalysts

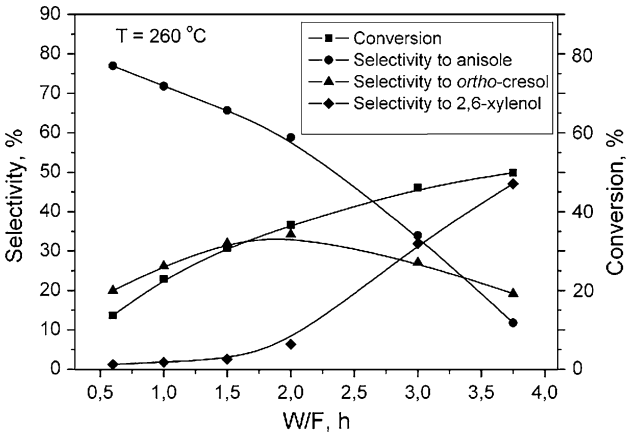

Fig. 8 Contact time dependence of phenol conversion and selectivities to anisole, *ortho*-cresol and 2,6-xylenol for ZCAO catalyst at 260 °C

Two independent methods were adopted to evaluate the acidic and basic properties of studied solids. TPD-NH_3 measurements were used to investigate total surface acidity and the acid strength distribution. The gas phase competitive reaction of CHOL (dehydration/dehydrogenation) over aluminate catalysts was studied in order to determine their acid–base character. Dehydration activity of the catalysts could be correlated with their surface acidity while dehydrogenation with basicity. The results of acidic properties of catalysts' surface measured by TPD-NH_3 indicated that the order of total acidity was: ZCAO > ZAO > CAO. ZCAO sample was mainly characterized by higher part of weak and strong acid sites (at $T_{des} < 300$ and > 500 °C, respectively), while ZAO and CAO by medium centres. The relationship observed for the activity in CHOL conversion was the same as mentioned above. All aluminate spinels exhibited good conversions yielding CHEN as the product of dehydration and CHON obtained during dehydrogenation. Aluminate spinel containing zinc and cobalt ions (ZCAO) showed a general increase in acidity and visible increase in dehydrogenation activity which meant that it was characterized by the most basic properties. It was accepted, that CHON/CHEN selectivity ratio gives information about basic nature of catalysts surface (see Table 2).

It is known that *ortho*-selectivity of phenol alkylation is governed by the type of phenol adsorption on the catalyst surface, depending on its acidic strength. For better results of *ortho*-alkylation toward the hydroxyl group of phenol catalyst used apart from acidic centres should also have basic ones because during reaction phenol molecule interacts with an acid–base pair sites, dissociatively adsorbing as a phenolate ion on the acid site while proton interacts with the adjacent basic site. The dissociated proton from phenol quite easy activates the molecule of methanol forming methyl carbocation. It has been reported, among others, by Mathew et al., that the activation of the reactant molecule is through its association with acid–base pair centres on metal oxide; this function plays an important role in the catalytic activity towards phenol conversion and desired product selectivity for any alkylation [37, 50]. On more basic catalysts the phenol molecule adsorbs vertically to the catalysts surface due to the repulsion between the highly nucleophilic O^{2-} surface anions and the aromatic ring. This behaviour of phenol molecules gives preference mainly to an attack of the methyl cation in the *ortho*-position, because these positions are the nearest to the catalyst surface. In this case C-methylated products can be obtained with high *ortho*-selectivity. Phenol takes a position oblique or parallel to the surface on more acidic catalysts' surface because acid centres interact with the π-electrons of the benzene ring of phenolate formed on the catalyst surface, which gets low probability of substitution in the *ortho* position. This model of phenol adsorption was proposed by Tanabe et al. [51] and widely accepted. It was found by Mathew et al. that methylated phenols had weak interaction with the surface of spinel-type materials in comparison with phenol and were highly susceptible to desorbing from the surface and just could facilitate efficient methylation on such systems [28]. We observed that acidity and catalytic activity were the highest when ZCAO as catalyst had been used.

The substitution of Co^{2+} for Zn^{2+} ions creates more acidic centres, as revealed from the NH_3 desorption and CHOL conversion studies. Stronger acid sites are required for secondary alkylation to yield 2,6-xylenol, whereas only weaker acid sites are needed for the formation of primary alkylation to yield *ortho*-cresol. The results which we have obtained show that on all catalysts besides C-methylated phenol derivatives also anisole (product of O-methylation) was simultaneously obtained. The last one was intermediate, because its yield decreased at higher temperatures. Under the influence of studied catalysts anisole is a reactive molecule and undergoes the rearrangement, giving *ortho*-cresol, and phenol as a demethylation product. The mechanism of this rearrangement we proposed earlier [49]. It must be stated that further work is still required in order to understand the real role of the spinel structure and surface acid–base properties on the catalytic performance of Zn and Co containing aluminates.

4 Conclusions

Microwave-assisted glycothermal method was successfully used to synthesise nanosized spinel type mixed oxide containing Al, Zn and/or Co ions. Nanocrystalline spinels are characterised by high surface area and mesoporous nature. Acid–base properties measured in the test of CHOL conversion indicate that $Zn_{0.5}Co_{0.5}Al_2O_4$ spinel possesses relatively more basic surface character than others ($ZnAl_2O_4$ or $CaAl_2O_4$) what may explain its higher selectivity to *ortho*-cresol formation. Simultaneously, the highest conversion of CHOL and the highest NH_3 desorption suggest that also acid centres are present on the surface of this samples what was reflected in high phenol conversion and 2,6-xylenol obtaining. Additionally, adsorption of phenol on acid sites can provide also to O-alkylation of phenol, but also could be responsible for *ortho*-cresol formation through the rearrangement of adsorbed anisole [49, 52]. It seems that these specific properties of $Zn_{0.5}Co_{0.5}Al_2O_4$ lead to the optimal ratio between acidic and basic character of this material surface what results in good catalytic performance for phenol methylation to *ortho*-methylated derivatives.

Acknowledgments This work is supported by Polish Committee for Scientific Research (Grant No. N N507 500738). The authors are very grateful to Mrs. Ludwina Krajczyk for HRTEM studies.

References

1. Valenzuela MA, Bosch P, Aguilar-Rios G, Montoya A, Schifter I (1997) J Sol–Gel Sci Technol 8:107
2. Calbo J, Tena MA, Monrós G, Llusar M, Badenes JA (2006) J Sol–Gel Sci Technol 38:167
3. Păcurariu C, Lazău I, Ecsedi Z, Lazău R, Barvinschi P, Mărginean G (2007) J Eur Ceram Soc 27:707
4. Grabowska H, Miśta W, Trawczyński J, Wrzyszcz J, Zawadzki M (2001) Res Chem Intermed 27:305
5. Grabowska H, Zawadzki M, Syper L, Miśta W (2005) Appl Catal A: Gen 292:208
6. Grabowska H, Zawadzki M, Syper L (2006) Appl Catal A: Gen 314:226
7. Grabowska H, Zawadzki M, Syper L (2008) Catal Lett 121:103
8. Tavangarian F, Emadi R (2010) J Alloy Compd 489:600
9. Zawrah MF, Hamaad H, Meky S (2007) Ceram Int 33:969
10. Wei X, Chen D (2006) Mater Lett 60:823
11. Staszak W, Zawadzki M, Okal J (2010) J Alloy Compd 492:500
12. Ouahdi N, Guillemet S, Demai JJ, Durand B, Er Rakho L, Moussa R, Samdi A (2005) Mater Lett 59:334
13. Gama L, Ribeiro MA, Barros BS, Kiminami RHA, Weber IT, Costa ACFM (2009) J Alloy Compd 483:453
14. Ifrah S, Kaddouri A, Gelin P, Leonard D (2007) C R Chimie 10:1216
15. Inoue M (2004) J Phys-Condens Matter 16:S1291
16. Santacesaria E, Grasso D, Gelosa D, Carrá S (1990) Appl Catal 64:83
17. Campelo JM, Garcia A, Luna D, Marinas JM, Moreno MS (1988) Stud Surf Sci Catal 41:249
18. Rao VV, Chary KVR, Durgakumari V, Narayanan S (1990) Appl Catal 61:89
19. Choi WC, Kim JS, Lee TH, Woo SI (2000) Catal Today 63:229
20. Cavani F, Maselli L, Passeri S, Lecher JA (2010) J Catal 269:340
21. Kotanigawa T, Yamamoto M, Shimokawa K, Yoshida Y (1971) Bull Chem Soc Jpn 44:1961
22. Grabowska H, Kaczmarczyk W, Wrzyszcz J (1989) Appl Catal 47:351
23. Grabowska H, Jabłoński J, Miśta W, Wrzyszcz J (1996) Res Chem Intermed 22:53
24. Samolada MC, Grigoriadou E, Kiparissides Z, Vasalos IA (1995) J Catal 152:52
25. Marczewski M, Perot G, Guisnet M (1996) React Kinet Catal Lett 57:21
26. Sad ME, Padró CL, Apesteguía CR (2008) Catal Today 133–135:720
27. Sreekumar K, Sugunan S (2002) J Mol Catal A: Chem 185:259
28. Mathew T, Shiju NR, Sreekumar K, Rao BS, Gopinath CS (2002) J Catal 210:405
29. Wolska J, Przepiera K, Grabowska H, Przepiera A, Jabłoński M, Klimkiewicz R (2008) Res Chem Intermed 34:43
30. Ballarini N, Cavani F, Passeri S, Pesaresi L, Lee AF, Wilson K (2009) Appl Catal A: Gen 366:184
31. Wang Y, Zhou Z, Jia M, Zhu X, Zhang W, Jiang D (2005) Catal Lett 104:67
32. Reddy AS, Gopinath CS, Chilukuri S (2006) J Catal 243:278
33. Wang Y, Yang P, Liu G, Jia M, Zhang W, Jiang D (2008) Catal Commun 9:2044
34. Lázár K, Mathew T, Koppány Z, Megyeri J, Samuel V, Mirajkar SP, Rao BS, Guczi L (2002) Phys Chem Chem Phys 4:3530
35. Mathew T, Tope BB, Shiju NR, Hedge SG, Rao BS, Gopinath CS (2002) Phys Chem Chem Phys 4:4260
36. Mathew T, Viayaraj M, Pai S, Tope BB, Hedge SG, Rae BS, Gopinath CS (2004) J Catal 227:175
37. Mathew T, Shylesh S, Devassy BM, Vijayarai M, Satyanarayana S, Rao BS, Gopinath CS (2004) Appl Catal A Gen 273:35
38. Grabowska H, Miśta W, Trawczyński J, Wrzyszcz J, Zawadzki M (2001) Appl Catal A: Gen 220:207
39. Miśta W, Zawadzki M, Grabowska H (2003) Res Chem Intermed 29:137
40. Grabowska H, Miśta W, Zawadzki M, Wrzyszcz J (2003) Polish J Chem Technol 5:32
41. Martin D, Duprez D (1997) J Mol Catal A: Chem 118:113
42. Sparks AK (1972) US Patent 3,670,030
43. Frabetti AF (1975) US Patent 4,041,085
44. Leach BE (1980) US Patent 4,227,024
45. Popović J, Tkalčec E, Gržeta B, Kurajica S, Rakvin B (2009) Am Mineral 94:771
46. Kim SS, Shah J, Pinnavaia TJ (2003) Chem Mater 15:1664
47. Triantafyllidis KS, Lapas AA, Vasalos IA, Liu Y, Wang H, Pinnavaia TJ (2006) Catal Today 112:33
48. Jacobs J-P, Maltha A, Reintjes JGH, Drimal J, Ponec V, Brongersma HH (1994) J Catal 147:294
49. Grabowska H, Zawadzki M, Syper L (2004) Appl Catal A: Gen 265:221
50. Kotanigawa T (1974) Bull Chem Soc Jpn 47:950
51. Tanabe K, Nishizaki T (1977) In: Bond GC, Wells PB, Tompkins FC (eds) Proc 6th Intern Congr Catal Chem, vol 12, London, p 863
52. Jacobs JM, Parton RF, Boden AM, Jacobs PA (1988) Stud Surf Sci Catal 41:221